IV International Conference on Computational Methods for Coupled Problems in Science and Engineering
COUPLED PROBLEMS 2011
M. Papadrakakis, E. Oñate and B. Schrefler (Eds)

REDUCED-ORDER MODELING OF PARAMETRIZED FINITE ELEMENT SOLUTIONS BY THE POD-ISAT TECHNIQUE. APPLICATION TO AIRCRAFT AIR CONTROL SYSTEMS

Dung Bui*, Mohamed Hamdaoui* and Florian De Vuyst†

* Mathematics Applied to Systems Lab,
Ecole Centrale Paris,
Grande Voie des Vignes, Châtenay-Malabry cedex, France
e-mail: dung.bui@ecp.fr, mohamed.hamdaoui@m4x.org, http://www.mas.ecp.fr/

† Center of Applied Mathematics and their Applications (CMLA)
Ecole Normale Supérieure de Cachan,
61, avenue du Président Wilson 94235 Cachan cedex
e-mail: devuyst@cmla.ens-cachan.fr, http://www.cmla.ens-cachan.fr/

Key words: Multiphysics Problems, Reduced-Order Modeling (ROM), nonintrusive, In-Situ-Adaptive-Tabulation (ISAT), Proper Orthogonal Decomposition, Aircraft air control system.

Abstract. A combined Proper Orthogonal Decomposition (POD) + In Situ Adaptive Tabulation (ISAT) is proposed for the representation of parameter-dependent solutions of coupled partial differential equations (PDE). The method is tested on a coupled fluid-thermal problem: the design of a simplified aircraft air control system. Furthermore, the control of the method's accuracy is discussed, leading to the metamodeling of the residual itself. The presented POD-ISAT approach provides by its flexibility and robustness an appropriate representation of the solutions for different use cases (sensitivity analysis, optimization, etc.)

1 Introduction

Computational tools are today a success factor in Engineering Design. Finite Elements or Finite Volumes codes become very efficient in the evaluation of criteria at given design points. However, the 'full' exploration of the design space is still a difficult task because of the curse of dimensionality and the weak computing performance available for such applications. Alternative solutions are the use of meta-models or low-order optimal bases that show both accuracy and computational efficiency for particular classes of problems (elliptic problems). Proper Orthogonal Decomposition (POD) [1], Reduced

Basis Method (RBM) [2, 3], LATIN methodology [4] or Proper Generalized Decompositions (PGD) [5] are among the most known computational approaches for dimensionality reduction of PDE solutions. But there are still big issues such as the case of hyperbolic problems, convection-dominated problems, strongly coupled multiphysics problems, high-dimensional design spaces, etc.
The present paper deals with the design of a simplified aircraft air control system depending on inflow and exterior conditions. Navier-Stokes equations are coupled with a thermal equation by means of a buoyancy force (Boussinesq approximation). In this work, an innovating approach called POD-ISAT is presented. It combines Proper Orthogonal Decomposition for the representation of the spatial fields and In Situ Adaptive Tabulation (ISAT) for the local representation of the solution in the design space. This leads to a set of local reduced-order models whose fidelity is controlled by means of trust regions (TR). In Pope's ISAT model [6, 7], ellipsoids of accuracy (EOA) are used and adapted during the learning process of the table. Here we rather use a threshold criterion on a residual. The whole algorithm is detailed in the paper and numerical results show the efficiency of the approach.

2 Mathematical setting

We are interested in the modelling of stationary air circulation and heating conditions in an aircraft cabin. For the sake of simplicity, the flow is supposed two-dimensional and the domain of interest is the cross-section of the fuselage (see figure 1). The air is seen as an incompressible fluid but we take into account buoyancy Archimedes forces due to air heating. So the stationary Navier-Stokes equations with the Boussinesq approximation are considered. At the right hand side of the Navier-Stokes momentum equation (2) appears a buoyancy term depending on the gravity $\boldsymbol{g}$ and the temperature deviation $(T - T_0)$ from the nominal temperature T_0. The Navier-Stokes equations are coupled, through this buoyancy term, with a thermal equation that governs the evolution of the temperature of the fluid (equations (1)-(3)). The coefficient κ is the thermal diffusivity of the air.

$$\nabla \cdot \boldsymbol{u} = 0 \quad \text{in } \Omega, \tag{1}$$

$$\boldsymbol{u} \cdot \nabla \boldsymbol{u} - \nu \Delta \boldsymbol{u} + \nabla p = \boldsymbol{g}\,(1 - \alpha(T - T_0)) \quad \text{in } \Omega, \tag{2}$$

$$\boldsymbol{u} \cdot \nabla T - \nabla \cdot (\kappa \nabla T) = 0 \text{ in } \Omega, \tag{3}$$

In realistic conditions, the reference length L is 1 m, the characteristic speed U if 1 m/s and the kinematic viscosity of the air at 300K is $1.57\,10^{-5}\ m^2/s$ so that the Reynolds number is equal to

$$Re = \frac{LU}{\nu} \approx 6.37\,10^4.$$

The flow regime is turbulent, but, for the sake of simplicity, we do not take into account any turbulence model. Moreover the thermal diffusivity of air at 300K and 1 atm is

$2.22\,10^{-5}\ m^2/S$, thus the Péclet number is

$$Pe = \frac{LU}{\kappa} \approx 4.52\,10^4.$$

Let us consider now the boundary conditions. The cabin boundary is denoted Γ. It is

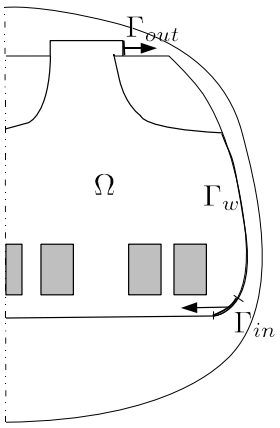

Figure 1: Spatial geometry and domain boundaries (half domain with symmetry axis)

divided into three parts: the inflow boundary Γ_{in}, the outflow Γ_{out} and the wall boundary Γ_w. For the fluid, no slip boundary conditions is used on Γ_w, velocity is imposed at the inflow and constant pressure is given at the outflow:

$$\boldsymbol{u} = 0 \text{ on } \Gamma_w,\ \boldsymbol{u} = \boldsymbol{u}_{in} \text{ on } \Gamma_{in} \text{ and } p = 0 \text{ on } \Gamma_{out}. \tag{4}$$

For thermal boundary conditions, we use Dirichlet boundary conditions on Γ_{in} with imposed inflow temperature T_{in}. The heat loss at the walls is expressed by inhomogeneous Fourier boundary conditions. The boundary heat flux may depend on the difference between the wall temperature and the exterior temperature. Finally, homogeneous Neumann boundary conditions are written at the outflow:

$$T = T_{in} \text{ on } \Gamma_{in},\ \frac{\partial T}{\partial n} = 0 \text{ on } \Gamma_{out},\ \kappa \frac{\partial T}{\partial n} = \Phi(T - T_{ext}) \text{ on } \Gamma_w. \tag{5}$$

Possibly, if interior boundaries are defined (like seats for example), then homogeneous Neumann boundary conditions are imposed. The whole system is non linear and the dominating phenomenon is the convection (because of the large Reynolds and Péclet numbers). It is assumed that the domain boundaries are Lipschitz continuous, $\boldsymbol{u}_{in}, T_{in} \in L^2(\Gamma_{in})$, $\Phi \in \mathcal{C}^\infty$, so that $(\boldsymbol{u}, p, T)$ are searched in $U_{u_{in}} \times L^2(\Omega) \times X_{T_{in}}$, where

$$U_w = \left\{ \boldsymbol{v} \in [H^1(\Omega)]^2,\ \boldsymbol{v} = 0 \text{ on } \Gamma_w,\ \boldsymbol{v} = \boldsymbol{w} \text{ on } \Gamma_{in} \right\},$$

$$X_w = \left\{ \tau \in H^1(\Omega),\ \tau = w \text{ on } \Gamma_{in} \right\}.$$

According to some approximate candidates $\tilde{\boldsymbol{u}} \in U_{u_{in}}$, $\tilde{p} \in L^2(\Omega)$ and $\tilde{T} \in X_{T_{in}}$, one can define a residual functional relative to the test functions $\boldsymbol{v} \in U_0$, $q \in L^2(\Omega)$ and $\tau \in X_0$:

$$R(\tilde{\boldsymbol{u}}, \tilde{p}, \tilde{T}, \boldsymbol{v}, q, \tau) = \int_\Omega (\tilde{\boldsymbol{u}} \cdot \nabla \tilde{\boldsymbol{u}}) \cdot \boldsymbol{v}\, dx + \int_{\Gamma_{out}} \frac{\partial \tilde{\boldsymbol{u}}}{\partial \boldsymbol{n}} \cdot \boldsymbol{v}\, d\sigma - \int_\Omega \tilde{p}\, \nabla \cdot \boldsymbol{v}\, dx$$
$$- \int_\Omega (1 - \alpha(\tilde{T} - T_0))\, \boldsymbol{g} \cdot \boldsymbol{v}\, dx + \int_\Omega \nabla \cdot \tilde{\boldsymbol{u}}\, q\, dx + \int_\Omega (\tilde{\boldsymbol{u}} \cdot \nabla \tilde{T}) \tau\, dx$$
$$- \int_\Omega \kappa\, \nabla \tilde{T} \cdot \nabla \tau\, dx - \int_{\Gamma_w} \Phi\, (\tilde{T} - T_{ext}) \tau\, d\sigma \quad \forall (\boldsymbol{v}, q, \tau) \in U_0 \times L^2(\Omega) \times X_0. \tag{6}$$

Parameters There are many parameters in the problem for which we would like to know the solutions of (1)-(5). Each parameter may vary in an interval. Among the parameter of interest, let us mention the exterior temperature T_{ext} (that naturally varies during the cruise), the inflow speed u_{in}, the inflow temperature T_{in}. Using dimensionless parameters $\theta_i \in [0, 1]$, $i = 1, \ldots, p$, we are looking for the family of fluid-thermal solutions $\big(\boldsymbol{u}^\theta = \boldsymbol{u}(\theta, .),\, T^\theta = T(\theta, .)\big)_{\theta \in [0,1]^p}$.

3 ROM methodology: general aspects and related works

A Reduced Order Model (ROM) for partial differential equations consists of a low-order representation of the solution by help of an 'optimal' basis and possibly an adaptivity and enrichment process. Considering for example the parameterized temperature field $\boldsymbol{u}^\theta = \boldsymbol{u}(., \theta)$, reduced-order are searched in the form

$$\boldsymbol{u}^\theta(x) = \boldsymbol{u}^{lift,\theta}(x) + \sum_{k=1}^{K} a_k(\theta)\, \boldsymbol{\Psi}^k(x). \tag{7}$$

The function $\boldsymbol{u}^{lift,\theta}$ is a lifting function aimed at satisfying some boundary conditions (especially Dirichlet BC), possible depending on θ but quite easy to compute (for example the solution of a linear Stokes Problem). The family $(\boldsymbol{\Psi}^k)_{k=1,\ldots,K}$ is the 'optimal' basis. The truncation rank K is expected to be rather small, let us say 10. The expansion coefficients $a_k(\theta)$ are functions depending on the vector parameter $\theta \in [0, 1]^p$. In a ROM methodology, there are two main steps: the design of the basis functions $\boldsymbol{\Psi}^k$ and the learning process of the $a_k(\theta)$.

In the POD snapshot approach [1, 8], some snapshot fields $(\boldsymbol{u}^i)_{i=1,\ldots,N}$ are computed according to a Design of Computer Experiment (DoCE). Then, the POD basis spawns the best linear subspace able to represent the snapshot solutions:

$$\min_{\substack{(\boldsymbol{\Psi}^1, \ldots, \boldsymbol{\Psi}^K) \\ (\boldsymbol{\Psi}^k, \boldsymbol{\Psi}^\ell) = \delta_{k\ell},\ 1 \le k \le \ell \le N}} \frac{1}{2} \sum_{i=1}^{N} \left\| \boldsymbol{u}^i - \sum_{k=1}^{K} (\boldsymbol{u}^i, \boldsymbol{\Psi}^k)\, \boldsymbol{\Psi}^k \right\|^2. \tag{8}$$

In the POD methodology, the $(\mathbf{\Psi}^k)$ are said to be an empirical basis because of the empirical choice of the snapshot set (see [9] for a recent analysis on the optimal location of the snapshots). Reduced Basis Methods or RBM [2, 3] are more rigorous approaches where the basis is enriched during an iterative learning process. At a given iteration (k) involving k modes, a $(k+1)th$ mode Ψ^{k+1} is searched as a best corrector direction corresponding to the the worst case location in the parameter domain. This is a kind of 'min-max' algorithm. RBM involves easy-to-compute accuracy estimators; we refer to the literature ([10, 11, 12]) for this issue. Because of the iterative enrichment process, RBM belongs to the family of greedy algorithms. Let us emphasize that the RBM analysis framework is restricted to elliptic problems. Another and recent approach which knowns an increasing interest is the Proper Generalized Decomposition or PGD pioneered by Ladevèze and Chinesta and since extended and used in many fields of applications ([5, 13, 14, 15, 16, 17]). PGD is also a greedy algorithm where the variables are separated. From a level-k model $\tilde{\boldsymbol{u}}^{(k)}(\theta,.)$, a higher-fidelity model $\tilde{\boldsymbol{u}}^{(k+1)}(\theta,.)$ in the form

$$\tilde{\boldsymbol{u}}^{(k+1)}(\theta,.) = \tilde{\boldsymbol{u}}^{(k)}(\theta,.) + a_1^{(k+1)}(\theta_1)\, a_2^{(k+1)}(\theta_2) \ldots a_p^{(k+1)}(\theta_p)\, \mathbf{\Psi}^{(k+1)}(x), \tag{9}$$

where the one-dimensional functions $a_1^{(k+1)}(\theta_1)$, $a_2^{(k+1)}(\theta_2)$ $\ldots$ $a_p^{(k+1)}(\theta_p)$ and the spatial model $\mathbf{\Psi}^{(k+1)}(x)$ are searched in an optimal way, for example by a variational principle and a Galerkin projection, see references [5, 18] for more details. Although very promising, PDG still needs investigation especially for parameter problems. It is unclear from the numerical analysis point of view what is the truncation rank K for a given error criterion. Moreover, PGD for the moment is an intrusive approach, what can be a shortcoming in a practical industrial context. PGD also needs more developments in the case of coupled problems. In what follows, we are going to present the POD-ISAT methodology which is an easy-to-implement non-intrusive approach that can be used in an industrial context.

4 The POD-ISAT algorithm

The determination of POD modes by the method of snapshots [1] relies on the computation of some accurate finite element solutions. A very popular physics-based metamodeling technique, namely the POD-Galerkin approach, consists in carrying out the approximation on the full Finite Element vector fields using POD modes and Galerkin projection [19]. Nevertheless, the main drawback of this method is its intrusive feature: the computational code has to be modified in order to develop a ROM. Besides, the resulting system of ODEs can become unstable or chaotic, misrepresenting the physics [20]. In the present work, we expose a non-intrusive reduced order model based on the combination of the POD method with the famous ISAT algorithm [6, 7].

4.1 Design of Computer Experiment(DoCE)

The parameter space sampling has an important impact on the metamodels accuracy. Commonly used DoCE procedure include Latin Hypercube Sampling (LHS), U-

designs [21] and Lattice Design [22]. A comparison of these methods [23], showed that the Lattice Design method outperforms the two other methods regarding the minimum distance criterion. Let N_{exp} be the number of design sites in the parameter space chosen according to a lattice design procedure. After computing the exact solutions (e.g. the temperature fields) for these design sites by a FE code, an initial snapshot set $\mathcal{S}^{N_{exp}}$ is formed as follows:

$$\mathcal{S}^{N_{exp}} = \left\{ u_0^i,\ i = 1, \ldots, N_{exp} \right\}. \tag{10}$$

4.2 The ISAT algorithm

The purpose of the ISAT algorithm is to tabulate a function $f(x)$, where x and f are of dimension n_x and n_f, respectively. Given a query, x_q, ISAT returns $f^a(x_q)$, an approximation to $f(x_q)$. An essential aspect of ISAT is that the table is built up, not in a pre-processing stage, but in situ (or "on line") as the simulation is being performed.

4.3 Local form of the POD-ISAT ROM

Assume that the current query parameter θ^i becomes a new entry for the table, say the ith entry. The corresponding solution $\boldsymbol{u}^i$ (e.g. temperature field) is computed by the FE model. Then a local reduced order model is built up at θ^i. This local model consists of an approximate model $\tilde{\boldsymbol{u}}_{(i)}(\theta)$ and a region of accuracy (ROA), denoted by $\mathcal{E}(i)$. The initial snapshot set $\mathcal{S}^{N_{exp}}$ is used to build a local snapshot set of N_{local} solutions that are centred with respect to $\boldsymbol{u}^i$ as follows:

$$\mathcal{S}_{(i)}^{N_{local}} = \left\{ \boldsymbol{u}_0^j - \boldsymbol{u}^i,\ j = 1, \ldots, N_{local} \right\}. \tag{11}$$

Then $K \leq N_{local}$ local POD modes $\boldsymbol{\Psi}_i^k\, k \in [1, \ldots, N_{local}]$ are computed using this local snapshot set and the local reduced order model $\tilde{\boldsymbol{u}}_{(i)}^{\theta}$ reads as follows:

$$\tilde{\boldsymbol{u}}_{(i)}^{\theta}(x) = \boldsymbol{u}_{(i)}^{lift,\theta}(x) + \sum_{k=1}^{K} a_{(i)}^k(\theta)\, \boldsymbol{\Psi}_{(i)}^k(x). \tag{12}$$

where the local POD coefficients $a_{(i)}^k$ depend on the parameters θ et θ^i.

4.4 Trust region

For $\theta = \theta^i$, provided that $\forall k \in [1, \ldots, K]$, $a_k(\theta_i) = 0$, we have $\tilde{\boldsymbol{u}}(., \theta^i) = \boldsymbol{u}(., \theta^i)$. Since the POD coefficients are supposed to be continuous, there is a region $\mathcal{E}(i)$, called trust region, such that the residual field satisfies

$$\forall \theta \in \mathcal{E}(i) \quad \|R(\tilde{\boldsymbol{u}}_{(i)}(\theta))\|_{\mathcal{L}^2}^2 \leq \varepsilon_{tol}^2,$$

with $\varepsilon_{tol} \ll 1$. The trust region $\mathcal{E}(i)$ is approximated by an ellipsoid [6] in $\mathbb{R}^p$ which is defined by $\frac{p^2+p}{2}$ unknown coefficients. The trust region is built by finding out $M > \frac{p^2+p}{2}$ different θ^* next to θ^i such as $|\|R(\theta^*)\|_{\mathcal{L}^2}^2 - \varepsilon_{tol}^2|$ is minimal. To tackle this problem, θ^*

is searched in the form $\theta^* = \theta^i + \alpha^* h$, with $\alpha^* \in \mathbb{R}$ and $h \in \mathbb{R}^p$ a fixed unit vector. By choosing M different vectors h, M vectors θ_h^* are computed in parallel on a multi-core machine as the M minimization runs are independent. Then, the M vectors θ_h^* are used to determine an ellipsoid of accuracy (EOA) using Ellipsoidal Toolbox [1]. The size of the EOA depends obviously on the choice of ε_{tol}.

4.5 POD-ISAT algorithm

Initially, the POD coefficients $a_{(i)}^k(\theta)$, $k \in [1, \ldots, K]$ (see (12)) are not known, however we have:

$$a_{(i)}^k(\theta^j) = (\boldsymbol{u}(x, \theta^j), \boldsymbol{\Psi}_{(i)}^k(x)); k = 1, \ldots, K; j = 1, \ldots, N_{local}. \tag{13}$$

Using (13), the coefficients $a_{(i)}^k(\theta)$ can be interpolated or approximated by standard robust methods (Moving Least Square (MLS) [24, 25], artificial neural networks (ANN) [26], radial basis functions (RBF) [27] or Kriging approaches).
In this paper, the coefficients $a_{(i)}^k(\theta)$ are determined by minimizing the $\mathcal{L}^2$ norm of the residual:

$$(a_{(i)}^1, \ldots, a_{(i)}^K)(\theta) = \arg \min_{(a_{(i)}^1, \ldots, a_{(i)}^K)} \frac{1}{2} \parallel R \left(\boldsymbol{u}_{(i)}^{lift,\theta}(x) + \sum_{k=1}^{K} a_{(i)}^k(\theta)\, \boldsymbol{\Psi}_{(i)}^k(x) \right) \parallel_{\mathcal{L}^2}^2 . \tag{14}$$

The optimization problem (14) is formulated in a low-dimensional space and is easy to solve. As initial guesses $a^k(\theta^i) = 0$, $k \in [1, \ldots, K]$ are used, but one can also use interpolated POD coefficients.
Once the $\mathcal{E}(i)$ for θ^i is determined, a sampling $(\theta^j)_{j=1,\ldots,M} \in \mathcal{E}(i)$ is generated and the POD coefficients $a_k(\theta^j)$, $k \in [1, \ldots, K]$, $j \in [1, \ldots, M]$ are computed by minimizing the residual (see (14)). Then, using these coefficients, a kriging interpolation model of $a_k(\theta)$ is built. Thus, the local ROM at point θ^i is completely defined by the EOA characteristics and the kriging interpolation model which are added to the table which is enriched adaptively allowing to cover the design domain [7]. The POD-ISAT algorithm is summarized in Fig 2.

5 Numerical results

Table 1 shows all the control parameters that impact the quality of the POD-ISAT ROM. The most important is ε_{tol} which controls the threshold error of the ROM. Some exact solutions computed with the FE model are plotted in figure 3. The significant CPU costs are outlined in Table 2. The speed-up, defined as the ratio of the time to evaluate a solution with the FE code by the time needed to compute a solution with the ROM, is $1000/0.6 \sim 1700$, which shows the efficiency of the POD-ISAT algorithm. A 100 random

[1] `http://www.mathworks.com/matlabcentral/fileexchange/21936-ellipsoidal-toolbox-et`

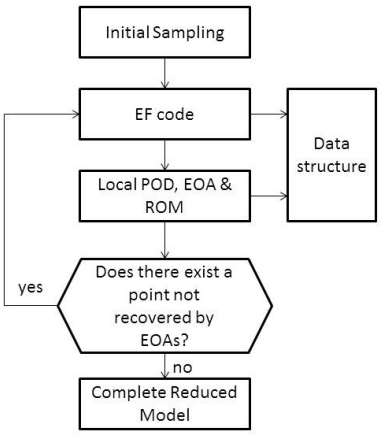

Figure 2: Schematic of the POD-ISAT algorithm

Table 1: Properties of reduced model

N_{exp}	60	Initial DoCE Size
ε^2_{tol}	$5\,10^{-10}$	Tolerance
N_{local}	10	Number of nearest neighbours for local POD
K	5	Number of POD modes used
p	3	Number of parameters

parameters vectors $\theta^i, i = 1, \ldots, 100$ are drawn in the parameter space. Then, the ROM is compared with the FE model using the following error formula:

$$relative \;\; error = \frac{\|\tilde{\boldsymbol{u}}(\theta) - \boldsymbol{u}(\theta)\|_{\mathcal{L}^2}}{\|\boldsymbol{u}(\theta)\|_{\mathcal{L}^2}}. \tag{15}$$

In Figure 4, where each color represents an EOA, we can see that the mean relative error is about 0.3% an that the maximum relative error is attained for the solution corresponding to $\theta^{12}(1.2\%)$. Furthermore, θ^{12}, θ^{70}, θ^{81} and θ^{57} are in the same EOA (they have the same color), which shows that their EOA was the worst defined because it is too large and inaccurate. Figure 5 shows the temperature fields of θ^{12} obtained by both reference model and reduced model. In order to better see the difference between both temperature fields, the difference in absolute value is plotted in Fig. 6.

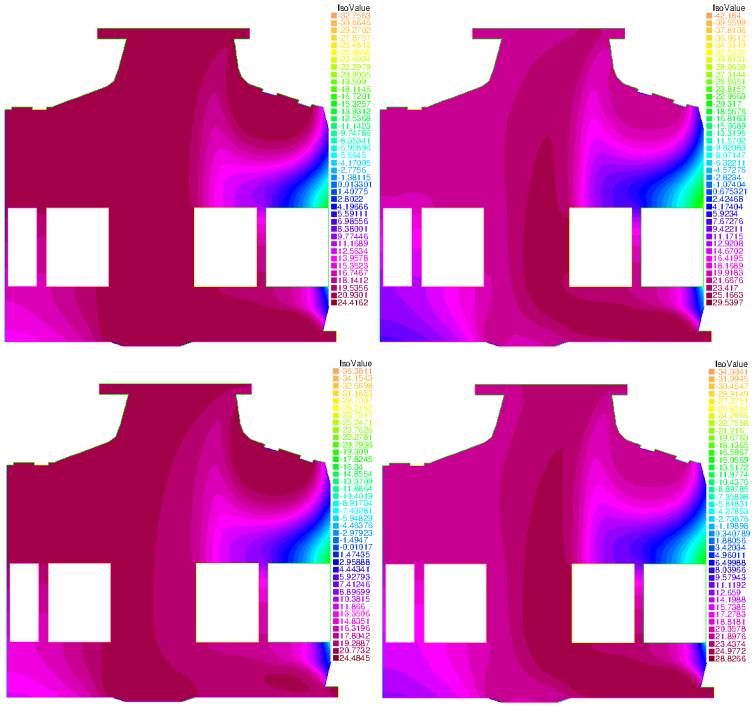

Figure 3: Reference FE solutions for different parameter samples.

	Online	Outline
EOA Building		1200 sec
Kriging model		300 sec
FE computation of $u(x, \theta)$		1000 sec
Retrieve	0.17 sec	
FE computation of $u^{lift}(x, \theta)$	0.43 sec	

Table 2: CPU costs

6 Concluding remarks

In this paper a non intrusive adaptive ROM combining POD and ISAT has been presented on the design of an aircraft control system. The numerical results show that the ROM is both efficient and accurate. However, the EOA can be inaccurately defined and as pointed out by [7] this problem can be tackled by adding an ellipsoid of inaccuracy or EOI around an EOA to control the inaccuracy of the EOA. Furthermore, the ε_{tol} controls the error on the residual and not on the solution itself which is not convenient,

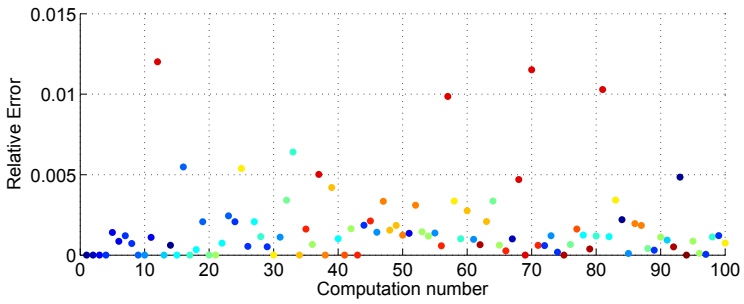

Figure 4: Relative errors for 100 random computations

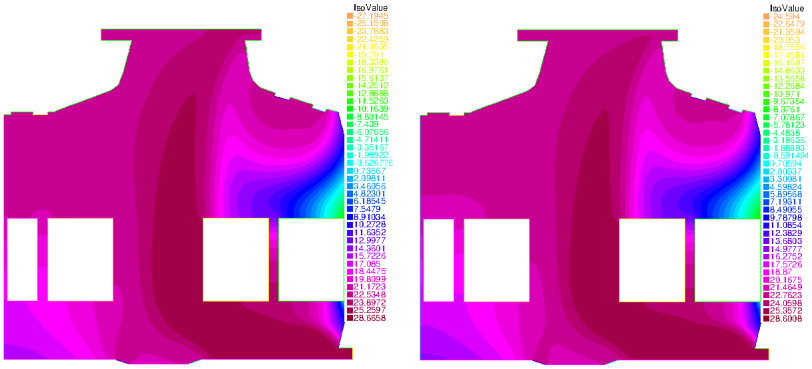

Figure 5: Solution of parameter θ^{12} for both reference model(left) and reduced model(right)

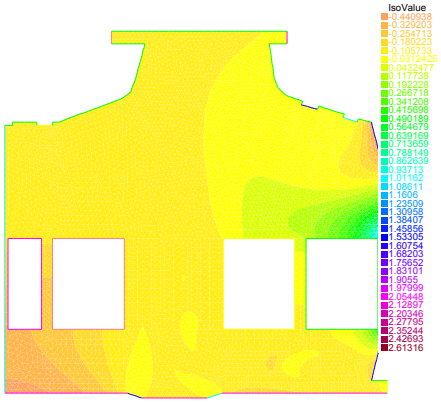

Figure 6: The error field for sample θ^{12} between the reference model and reduced model (°C)

which points out the need to consider different approaches to define the error.

Acknowledgements. This work is supported by the industrial platform 'Complex System Design Lab' CSDL, Pôle de Compétitivité System@tic, Paris Région Ile-de-France.

REFERENCES

[1] G Berkooz, P Holmes, and JL Lumley. The proper orthogonal decomposition in the analysis of turbulent flows. *Annual review of fluid mechanics*, 25:539–575, 1993.

[2] Yvon Maday and Einar M. Ronquist. A reduced-basis element method. *Comptes Rendus Mathématique*, 335(2):195 – 200, 2002.

[3] G. Rozza, D. Huynh, and A. Patera. Reduced basis approximation and a posteriori error estimation for affinely parametrized elliptic coercive partial differential equations. *Archives of Computational Methods in Engineering*, 15:229–275, 2007. 10.1007/s11831-008-9019-9.

[4] Ladevèze Pierre. *Nonlinear Computational Structural Mechanics. New Approaches and Non-Incremental Methods of Calculation*. Mech. Eng. Series. Springer-verlag, 2009.

[5] A. Ammar, B. Mokdad, F. Chinesta, and R. Keunings. A new family of solvers for some classes of multidimensional partial differential equations encountered in kinetic theory modeling of complex fluids. *Journal of Non-Newtonian Fluid Mechanics*, 139(3):153 – 176, 2006.

[6] S.B. Pope. Computationally efficient implementation of combustion chemistry using in situ adaptive tabulation. *Combustion Theory and Modelling*, 1(1):41–63, 1997.

[7] Liuyan Lu and Stephen B. Pope. An improved algorithm for in situ adaptive tabulation. *Journal of Computational Physics*, 228(2):361 – 386, 2009.

[8] F. De Vuyst. *Multidisciplinary Design Optimization in Computational Mechanics*, chapter PDE Metamodeling using Principal Component Analysis. Wiley ISTE, April 2010.

[9] Kunisch, Karl and Volkwein, Stefan. Optimal snapshot location for computing pod basis functions. *ESAIM: M2AN*, 44(3):509–529, 2010.

[10] K. Veroy and A. T. Patera. Certified real-time solution of the parametrized steady incompressible Navier-Stokes equations: rigorous reduced-basis a posteriori error bounds. *International Journal for Numerical Methods in Fluids*, 47(8-9):773–788, 2005.

[11] Gianluigi Rozza and Karen Veroy. On the stability of the reduced basis method for Stokes equations in parametrized domains. *CMAME*, 196(7):1244 – 1260, 2007.

[12] Simone Deparis. Reduced basis error bound computation of parameter-dependent Navier-Stokes equations by the natural norm approach. *SIAM J. Num. A.*, 46(4):2039–2067, 2008.

[13] A. Dumon, C. Allery, and A. Ammar. Proper general decomposition (pgd) for the resolution of Navier-Stokes equations. *Journal of Computational Physics*, 230(4):1387 – 1407, 2011.

[14] F. Chinesta, A. Ammar, A. Leygue, and R. Keunings. An overview of the proper generalized decomposition with applications in computational rheology. *Journal of Non-Newtonian Fluid Mechanics*, In Press, Corrected Proof:–, 2011.

[15] G. Bonithon, P. Joyot, F. Chinesta, and P. Villon. Non-incremental boundary element discretization of parabolic models based on the use of the proper generalized decompositions. *Engineering Analysis with Boundary Elements*, 35(1):2 – 17, 2011.

[16] A. Leygue and E. Verron. A first step towards the use of proper general decomposition method for structural optimization. *ACME*, 17:465–472, 2010. 10.1007/s11831-010-9052-3.

[17] M. Beringhier, M. Gueguen, and J. Grandidier. Solution of strongly coupled multiphysics problems using space-time separated representations. application to thermoviscoelasticity. *Arch. of Comp. Methods in Engineering*, 17:393–401, 2010. 10.1007/s11831-010-9050-5.

[18] Anthony Nouy. A priori model reduction through proper generalized decomposition for solving time-dependent partial differential equations. *Computer Methods in Applied Mechanics and Engineering*, 199(23-24):1603 – 1626, 2010.

[19] K. Kunisch and S. Volkwein. Galerkin proper orthogonal decomposition methods for a general equation in fluid dynamics. *SIAM J. on Numerical Analysis*, 40(2):492–515, 2002.

[20] A. Iollo, S. Lanteri, and J.-A. Désidéri. Stability properties of pod-galerkin approximations for the compressible Navier-Stokes equations. *Theoretical and Computational Fluid Dynamics*, 13:377–396, 2000. 10.1007/s001620050119.

[21] B. Tang. Orthogonal array-based latin hypercubes. *J. Am. St. Asso.*, (88):13921397, 1993.

[22] P. Winker K.T. Fang, D.K.J. Lin and Y. Zhang. Uniform previous termdesignnext term: theory and application. *Technometrics*, (42):237248, 2000.

[23] Dizza Bursztyn and David M. Steinberg. Comparison of designs for computer experiments. *Journal of Statistical Planning and Inference*, 136(3):1103 – 1119, 2006.

[24] P. Lancaster and K. Salkauskas. Surfaces Generated by Moving Least Squares Methods. *Mathematics of Computation*, 37(155):141–158, 1981.

[25] Piotr Breitkopf, Hakim Naceur, Alain Rassineux, and Pierre Villon. Moving least squares response surface approximation: Formulation and metal forming applications. *Computers & Structures*, 83(17-18):1411 – 1428, 2005. Advances in Meshfree Methods.

[26] Dreyfus Gérard. *Neural networks: methodology and applications*. Editions Eyrolles, 2005.

[27] C. Audouze, F. De Vuyst, and P. B. Nair. Reduced-order modeling of parameterized pdes using time-space-parameter PCA. *IJNME*, 80(8):1025–1057, 2009.